

## Seismic Reprocessing: Case Study Barrut Arch, Concession 72, Sirt Basin, Libya

Ali Abuagela, and Naji Miladi\*

### دراسة حالة إعادة المعالجة السيزمية لقوس باروت بعقد الامتياز رقم 72 بحوض سرت، ليبيا

علي أبو عجيبة وناجي الميلادي

تم إختيار البيانات التي تم مسحها عام 1999 ف لاختبار فاعلية إعادة معالجة البيانات السيزمية بمنطقة قوس باروت شمال غربي عقد الامتياز 72 لغرض إعادة المعالجة حيث أوضحت المعالجة الأصلية للمقاطع السيزمية ضعفا في نوعية البيانات وذلك من خلال صعوبة متابعة استمرارية الانعكاس السيزمي، خاصة مع وجود تصدعات بالمنطقة وهو ما زاد في صعوبة التفسيرات السيزمية. إن المشاركين في هذا المشروع قد عملا جنبا إلى جنب مع المعالج بصورة دائمة لاختيار أفضل الطرق في كل مرحلة من مراحل المعالجة الانسيابي. إن المقطع السيزمي النهائي الذي أعيدت معالجته قد أوضح تحسنا ملحوظا وخاصة في استمرارية الانعكاس السيزمي ووضوح التصدعات مقارنة بالمقطع الأصلي وبذلك تم تحاشي خيار تنفيذ برنامج مسح سيزمي جديد باهظ التكلفة.

**Abstract:** To test the benefits of reprocessing, 2D vibroseis data acquired in 1999 over the Barrut Arch in NW Concession 72 was selected for reprocessing. The original processed sections showed the data to be of poor quality where reflection continuity was difficult to follow. Also, the area is heavily faulted, which increased interpretation difficulties. The project participants worked with the processors on continuous bases in order to select the best parameters from each stage of the processing flow.

The final reprocessed seismic profiles illustrate significant improvement in horizon continuity and fault definition over the original processed data. The very expensive option of acquiring new seismic program was avoided.

## INTRODUCTION

Often older vintages of seismic data no longer meet the current requirements and geological objectives of exploration interpreters. When this stage is reached in an exploration project, the only options are to acquire new seismic program or reprocess the existing seismic database with the latest advanced techniques. Reprocessing is significantly more cost effective than the field acquisition of new seismic data. Processing methods in the areas of statics (signal-to-noise enhancement, frequency balancing, and migration) have advanced. Seismic data reprocessing, using state of the art techniques, should result in overall improvement in reflection detail, resolution, and frequency enhancement. Therefore, the reprocessed seismic data will be available for a more meaningful interpretation. Added attention to the statics solution, frequency balancing, and velocity corrections should help reduce or eliminate intersection misties. The objective was to improve horizon correlation and fault definition.

\* Veba Oil Operations - Tripoli , Libya.

### Geographical Setting

Concession 72 is located over the Ayn An Nagah Sub-Basin. This Sub-basin is the most southern in a series of sub-basins that together form the northwest trending Zallah Trough (Fig.1). The Zallah Trough is the major western component of the regional horst and graben structural fabric of the Sirt Basin (Johnson, 1992). The concession is subdivided into three blocks and is named from north to south; Barrut, Ayn An Nagah, and Al Abrag (Fig.1) (Johnson, 1992).

### Geological Setting

The Barrut Arch was structurally active during Oligocene to Post-Eocene. The arch had continued to rise through the Eocene and maintain its north-easterly trend on Concession 72. A fault reactivation occurred after the Eocene when the subsidence of the basin was at its maximum. These faults dissected the arch and cut across adjacent areas. The continued rise of the arch after this period of faulting caused additional displacement along faults which reached

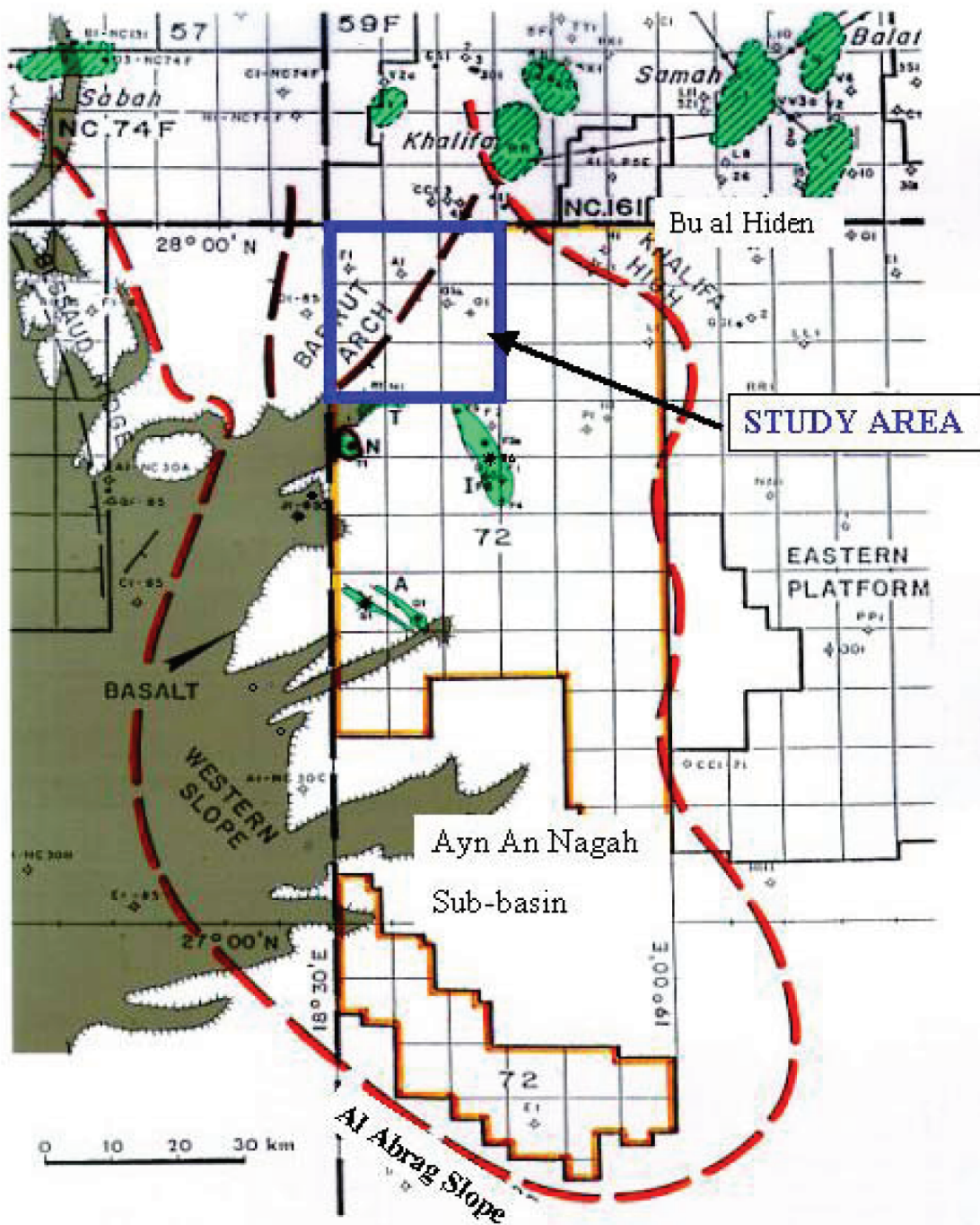


Fig. 1. Concession 72 location map showing Cretaceous boundaries of the Ayn An Nagah Sub-basin and the Barrut Arch.



or had influence further into the Ayn An Nagah Sub-basin. Some of these faults have a rotational or wrench-like character (Johnson, 1992). Additional faulting or fault adjustments may have accompanied the later igneous activity.

**Surface Geology**

The rocks and sediments exposed on Concession 72 range in age from Eocene to Recent. The oldest exposures are three outcrops of Eocene Gialo Formation located at the crest of the Barrut Arch in northwest Concession 72. The Barrut Arch is the only large scale structural feature exposed at the surface in Concession 72. Its southerly trending axis is two km west of well A1-72 where it then curves to the southwest off the concession. Oligocene and Miocene strata form escarpments which dip to the southeast and define portions of the arch’s south-eastern flank. Minor structural features, exposed at the surface on or near the arch, include northwest trending fault traces, a fracture zone and collapse structures. A shallow syncline runs parallel to the arch’s south-eastern flank between wells A1-72 and G1a-72.

Basalts are exposed at the surface in the Barrut Arch. The most prominent is a volcanic neck named Gleb el Barrut. It is located 5.2 km south-southwest of well A1-72 and is a radiating dike. Other intrusives, mostly dikes, occur at the surface in this area and have been described in some detail by Roadifer (1958), Geophoto Libya Inc. (1959), Johnson and Gates (1959), and Banar (1967).

**SEISMIC SURVEYS**

The seismic dataset in the Barrut Arch consists of 276.5 kms of regional 2D conventional seismic data of the surveyed lines acquired by VOO company in 1999 (Table 1). The data coverage is sparse over most of the Barrut Arch (Fig. 2). The quality of the data ranges from poor to good. Structural complexity and surface condition affects the data quality.

**Table 1. List of lines re-processed, Concession 72 NW, Barrut Arch area.**

Line	First VP	Last VP	First CDP	Last CDP	Length Kms	Direction
72-99-18	101	572	206	1142	18.840	SW-NE
72-99-19	101	781	206	1560	27.200	SW-NE
72-99-20	101	713	206	1424	24.480	NE-SW
72-99-21	101	454	206	905	14.120	SW-NE
72-99-22	101	701	206	1400	24.000	NW-SE
72-99-23	101	494	206	986	15.720	NW-SE
72-99-24	101	636	206	1270	21.400	NW-SE
72-99-25	101	856	206	1710	30.200	NW-SE
72-99-26	101	596	206	1190	19.800	NW-SE
72-99-27	101	531	206	1059	17.200	NW-SE
72-99-28	101	558	206	1114	18.280	NW-SE
72-99-29	101	464	206	926	14.520	NW-SE
72-99-30	101	387	206	772	11.440	NW-SE
72-99-31	101	583	206	1164	19.280	SW-NE
Total					276.48	

The acquisition parameters for this survey are summarized in Table 2 below.

**Table 2. Acquisition parameters, Concession 72 NW Barrut Arch.**

INSTRUMENTS		RECEIVERS		SOURCE	
Items	Specification	Items	Specification	Items	Specification
Type:	Sercel SN 388	Receiver type:	Sensor SM4-UB 10hz	Type of Vibrators:	Geco-Prakla V4 VVFB 50,000lbs
No. live receiver lines:	1	No. geophones/stn:	48(4stringsof12)	No. Vibrators:	5
No. live channels/line:	120	Pattern:	Rhomboidal	Sweep:	12-72 Hz log . (9db) Hi emphasis
Low cut filter:	Out	String separation:	5m	Sweep Length:	10sec
High cut filter	125 Hz	Geophone separation:	3.33 m	Taper:	300 ms cosine start and end
Sample rate:	2 ms	Overall pattern length:	51.6 m	Polarity:	SEG
Record length:	5000 ms	Overall pattern width:	15m	No. of sweeps/VP:	8 – phase rotated
Coverage	60	Overall pattern width:	40m	vibrators pattern:	Rhomboidal
Polarity:	SEG			Inline move up:	4 m
				Cross line spacing:	6 m
				Total pattern length	48 m
				Total pattern length	24 m
				Source station spacing:	40 m
				Spread parameters:	2500-140-0-140-2500 m

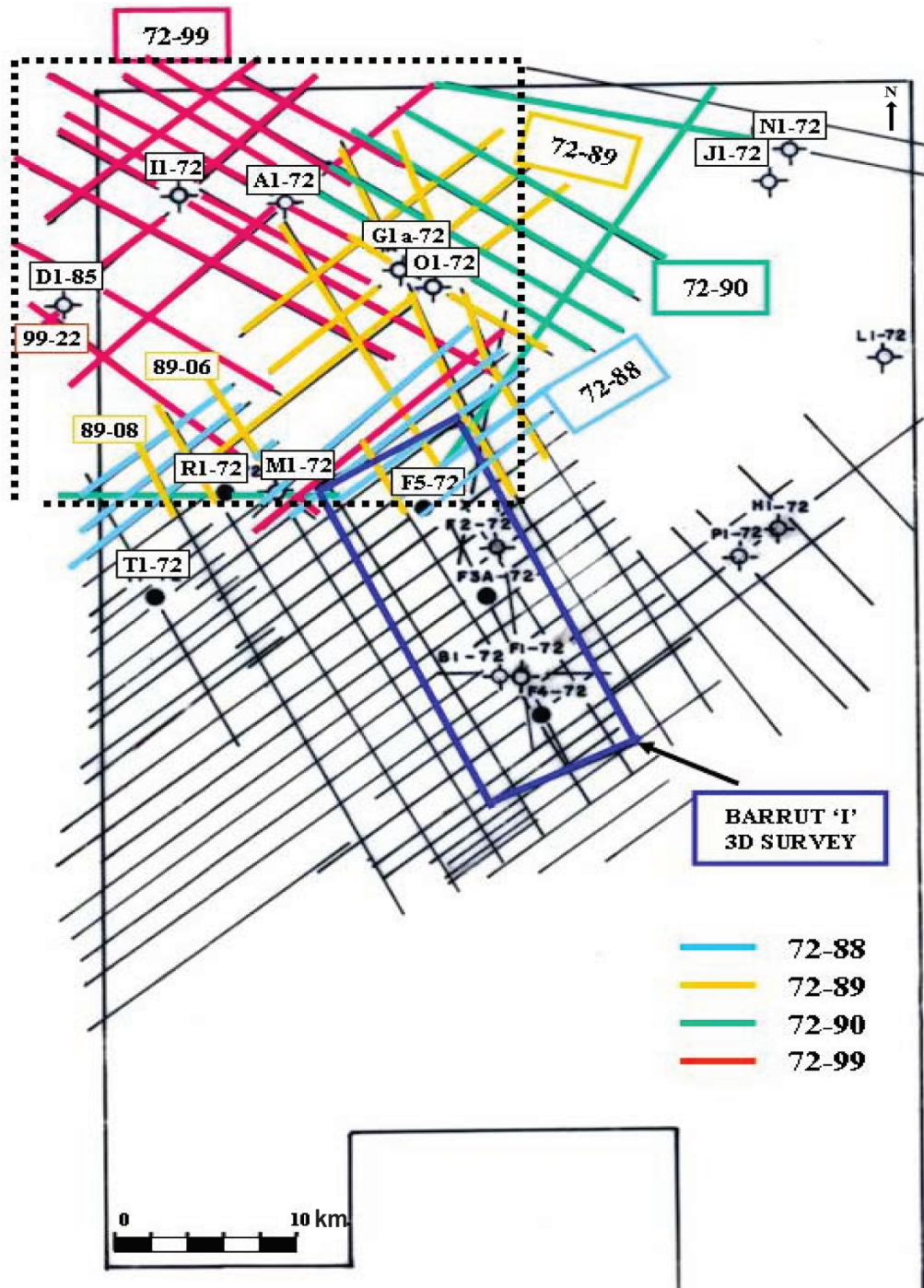


Fig. 2. Base map of Barrut Arch area, Concession 72.

**CURRENT PROCESSING**

Veba Oil Operations specified that the testing parameters should be performed on line 72-99-25. The summary of reprocessing test sequences are as follows:

- Parameter Testing**
- Preprocessing**
- Reformat**

The field data was received as 3480 cartridge

taps. The data was in SEG D (Society of Exploration Geophysicists) demultiplexed format of 5 second record length, and sampling rate of 2ms.

The seismic support data (navigation and geometry) was supplied as SPS (Shell Processing Support) format files on floppy diskettes.

**Geometry**

The navigation and spread details, provided in



survey (Shell) positioning system (SPS) files, were converted and loaded into internal format. This geometry information was then checked. These included surface and subsurface fold, source, receiver, and midpoint location points.

After applying the geometry to trace headers a number of checks were made to ensure that there is no geometry anomalies between the data and the SPS files.

**Data Editing**

Interactive trace editing was performed to edit out the isolated noisy and dead traces.

**Statics Calculation and Application**

Most of the QC (Quality Control) of refraction static has been performed using first-break stacks of the dominant refractor after LMO (linear move out) correction (Fig. 3). The refractor velocity is averaged over each shot point-receiver vector, which entails a natural smoothing filter.

The first-break stack quality should be fair to good and its picking should closely approximate the average of the time-picks. First-break stacking is an efficient technique in many cases. This first-break stack inversion uses direct and reverse shooting with respect to the general direction of acquisition.

Two methods are used for computing refraction static. The first method uses model tomography and is known as GLI (Generalised Linear Inversion and Tomographic Inversion).

The second method is referred to as traveltimes decomposition and uses simplified tomography, beyond a simple averaging procedure. Each individual time-pick is decomposed into a source delay, a receiver delay and LMO terms. The Geophone cluster module follows the second method.

Once the geometry has been properly set up, launch the first-break stacking phase in two modes. Stacks are computed and displayed in their ring and pick the stacks. Traces were picked in the direct and reverse shooting.

Static corrections are computed from picks of the first arrivals of refraction stacks. Two stacks are

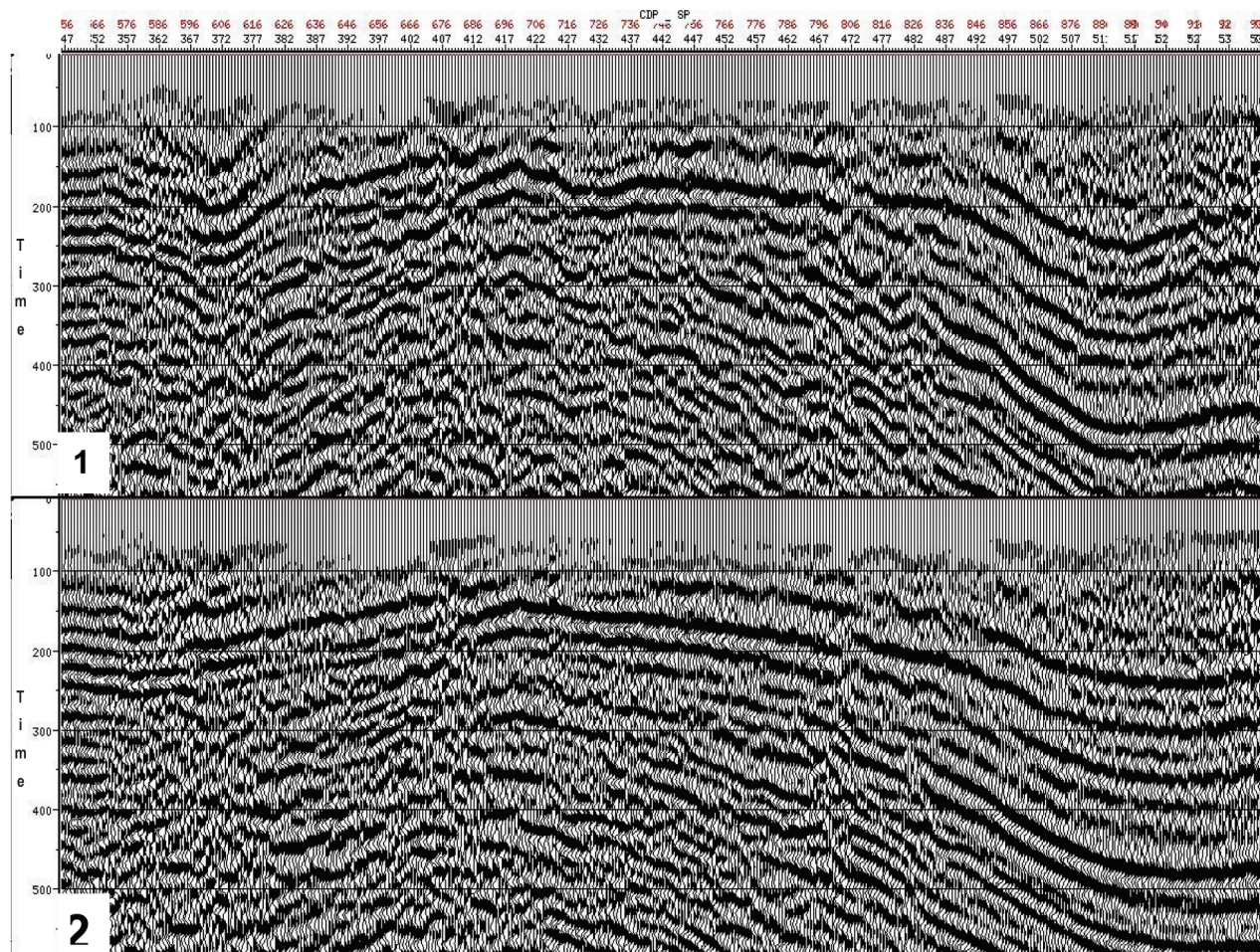


Fig. 3. Stack section showing: 1) stack with field statics, and 2) stack with refraction statics.



computed per source and receiver mode: direct and reverse stacks. Delays are computed for each point. Then, static corrections are computed from delays using weathering and refractor velocity parameters. Picking of elementary traces is used only with the computation of static and the result is saved in TDPIK or WXSTA format.

WXSTA is a program which computes static corrections from the times of the first break picks. The picking results from interactive applications, sorting and gathering of the picks allow construction of relative intercept curves which are handled according to the Gardner method.

Finally the statics were calibrated with the upholes, calculated and checked. The replacement velocity is used to correct from this pseudo datum to the final processing datum, in effect, a bulk shift in time. A replacement velocity of 2000 m/sec and a final datum of 200 m were used.

The result achieved, and the specific requirements to achieve the optimal result are shown below.

Although the first break pick quality was good, this area was characterized by some steeply dipping and discontinuous refractors, the statics application gave similar improvements (Fig. 3).

## PRESTACK PROCESSING

### Minimum phase conversion.

An auxiliary trace containing the filtered correlated pilot sweep was extracted. A minimum phase equivalent, a filter was calculated and applied to the seismic data.

### True Amplitude recovery

Spherical divergence gain functions were tested. The optimal result was decided as the application of  $T=V^2T$  (Fig. 4)

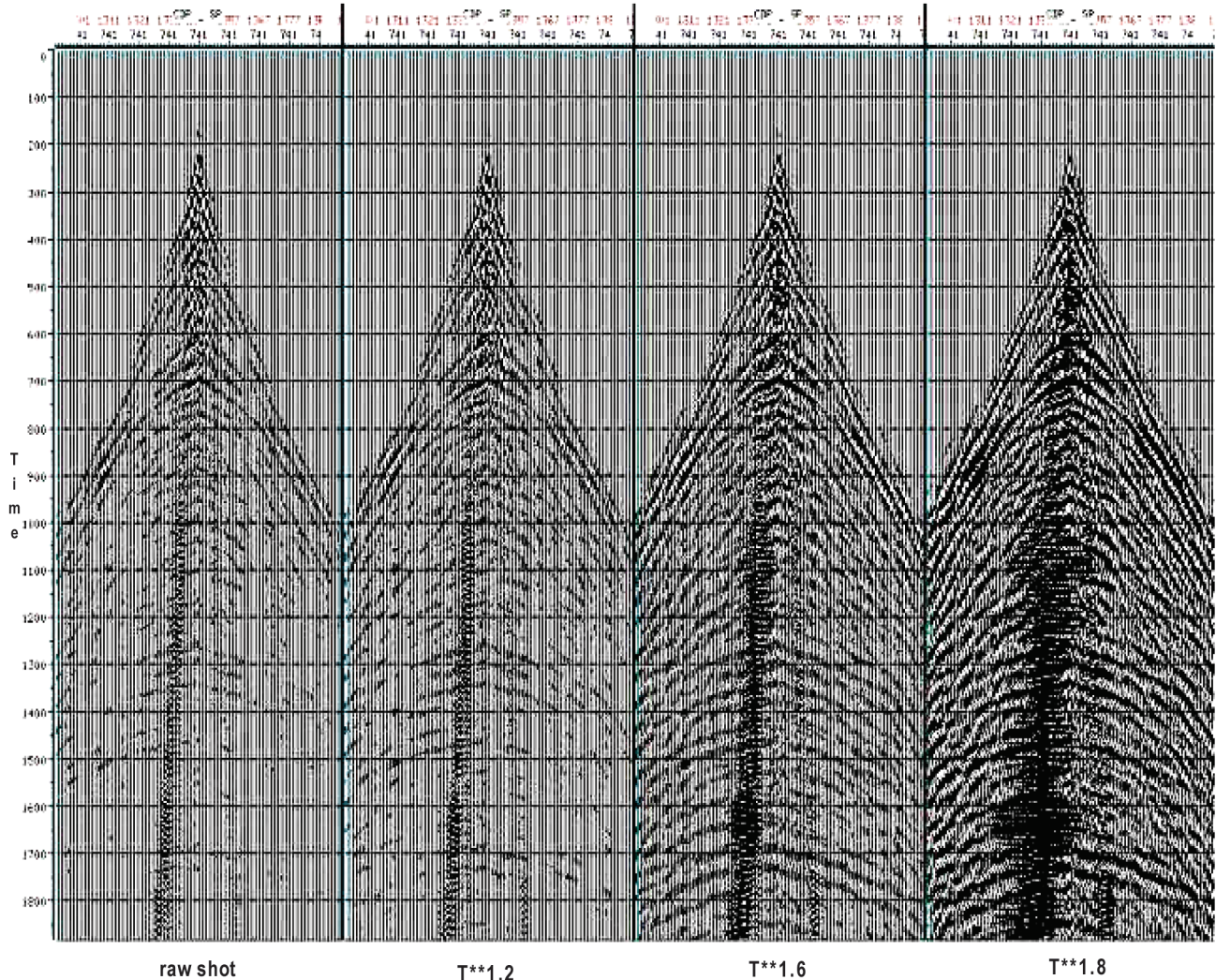


Fig. 4. Amplitude recovery.



**Noise Attenuation**

FK (frequency-wave number) filter test was performed with number of dips were tested to reduce a low frequency and spatially aliased groundroll. Plots were made of selected records, and the test lines stacked with the FK filter applied (Figs. 5a and 5b).

**Deconvolution Before Stack (DBS)**

Data was pre-processed with spherical divergence correction and (shot domain FK filtering applied. From the study of the above, the optimum operator length and predictive lag times were found. The test lines were then stacked using different DBS methods, ensemble DBS, one and two window trace DBS, and surface consistent DBS. The surface consistent DBS proved to give the best overall result (Fig. 6).

The final DBS parameters are: Surface consistent predictive deconvolution

Operator=160ms, lag=24ms, window: 0-1200ms

Operator=160ms, lag=12ms, window:

900-2400ms.

**Initial Velocity Analysis**

The initial or first pass velocity analysis was picked at 1km intervals using groups of 24 Common-midpoints (CMPs). The data was set to the near surface floating datum. The velocity were picked interactively, using constant velocity stacks, semblance, and gather displays is shown in Figure 7.

**Residual Statics**

The residual static program used is fully surface consistent medium and high frequencies. The analysis window was set to cover the maximum extent of good signal to noise (S/N) ratio data seen on the lines. The parameters for the residual statics applied are:

Window =200-2800 ms, maximum shift =15 ms, internal filter =12-55 Hz.

The residual statics typically provided very good short wavelength static control, and also solved for the longer wavelength static anomalies (Fig. 8).

**Prestack Partial Time Migration (DMO)**

The DMO used is a Kirchhoff-style based

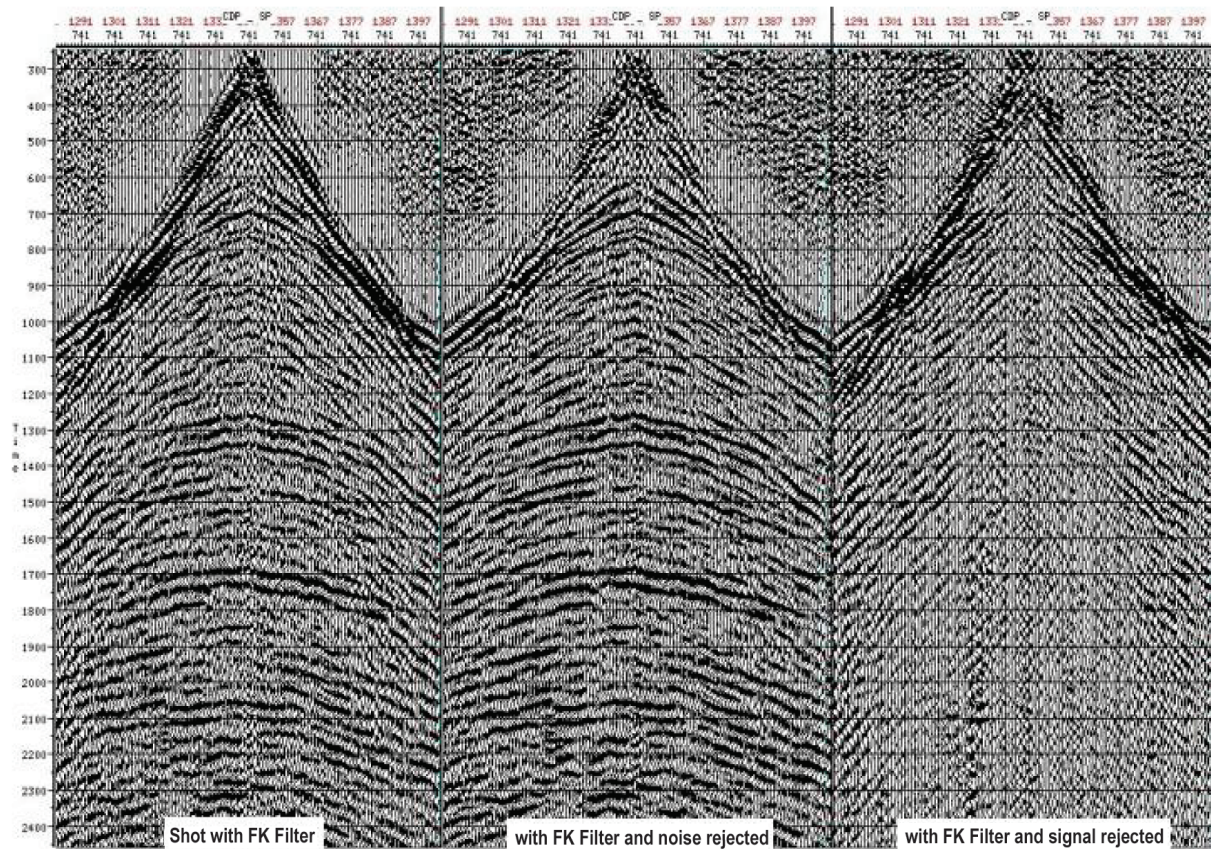


Fig. 5a. FK-filter full fan passing +/- 4000 ms.



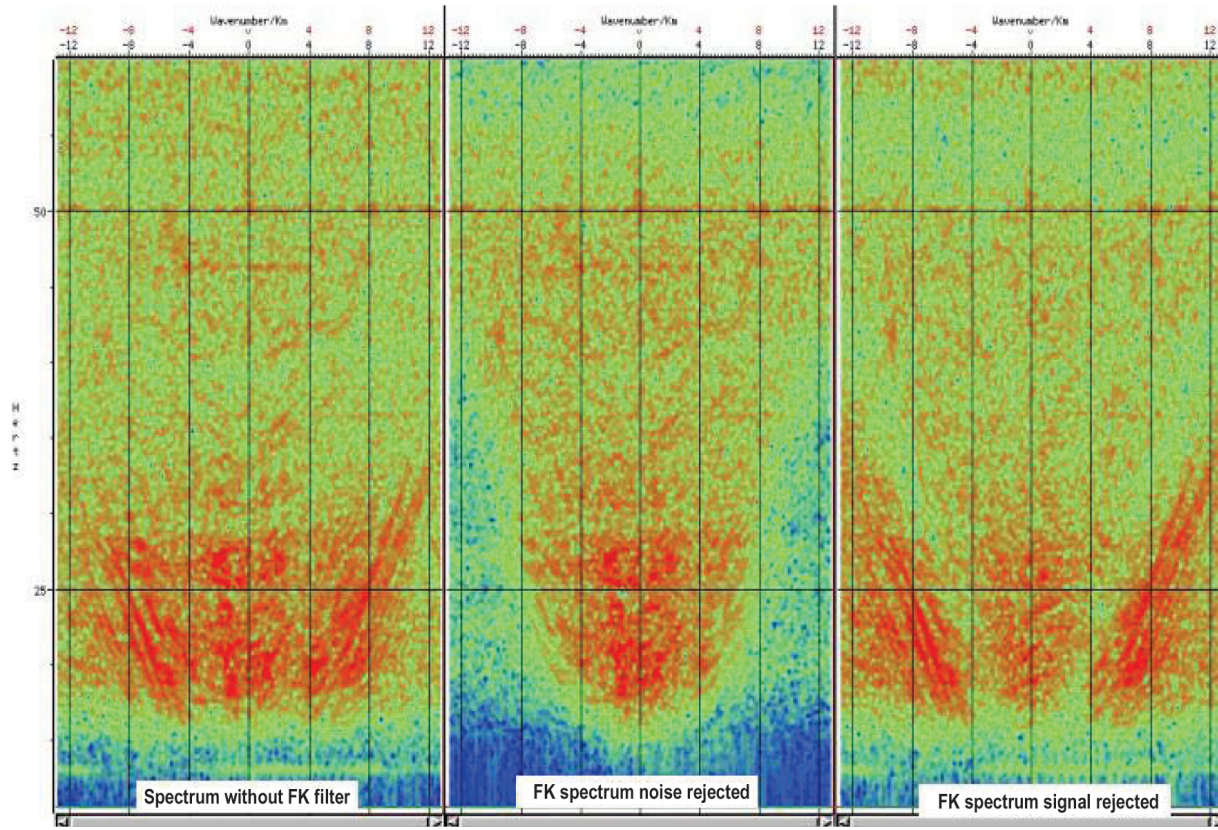


Fig. 5b. FK spectrum.

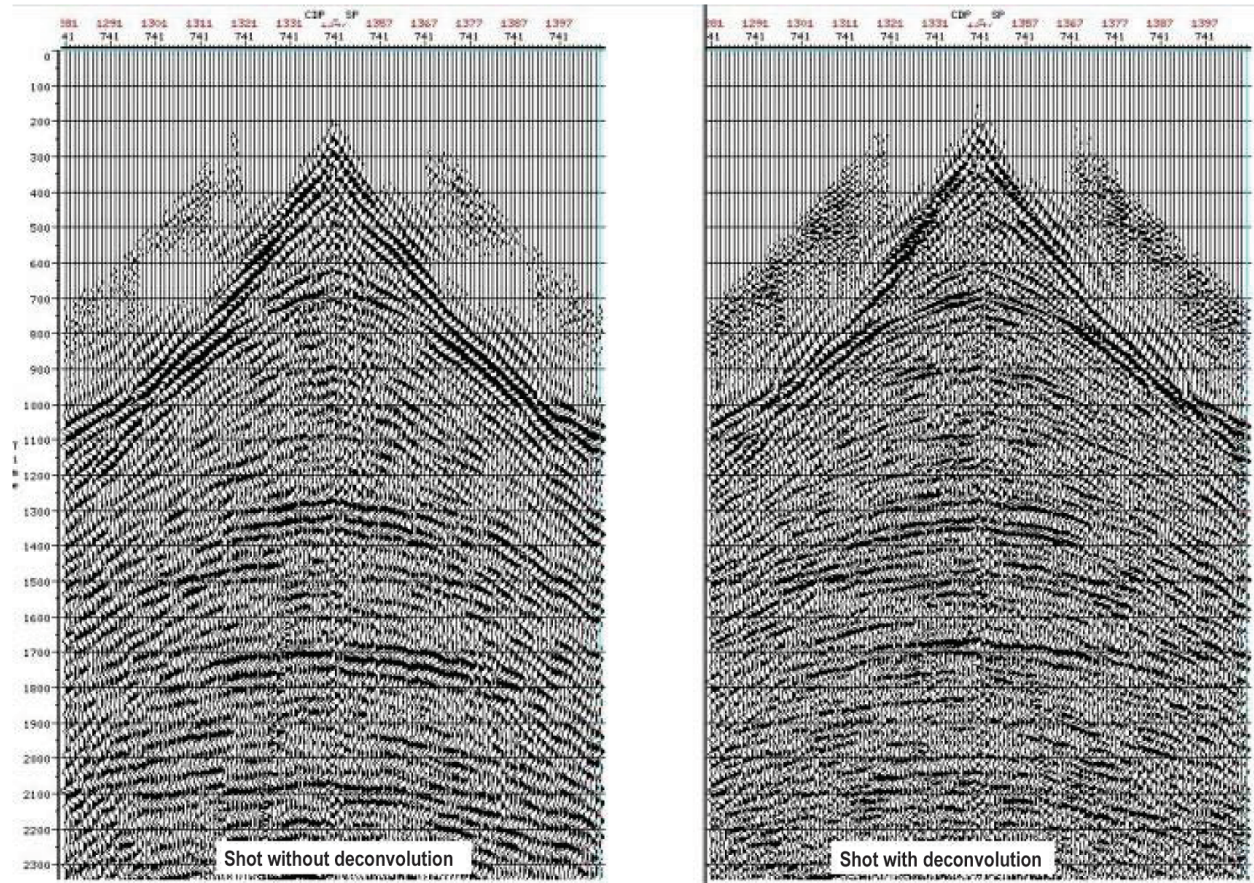


Fig. 6. Surface consistent deconvolution (predictive algorithm).



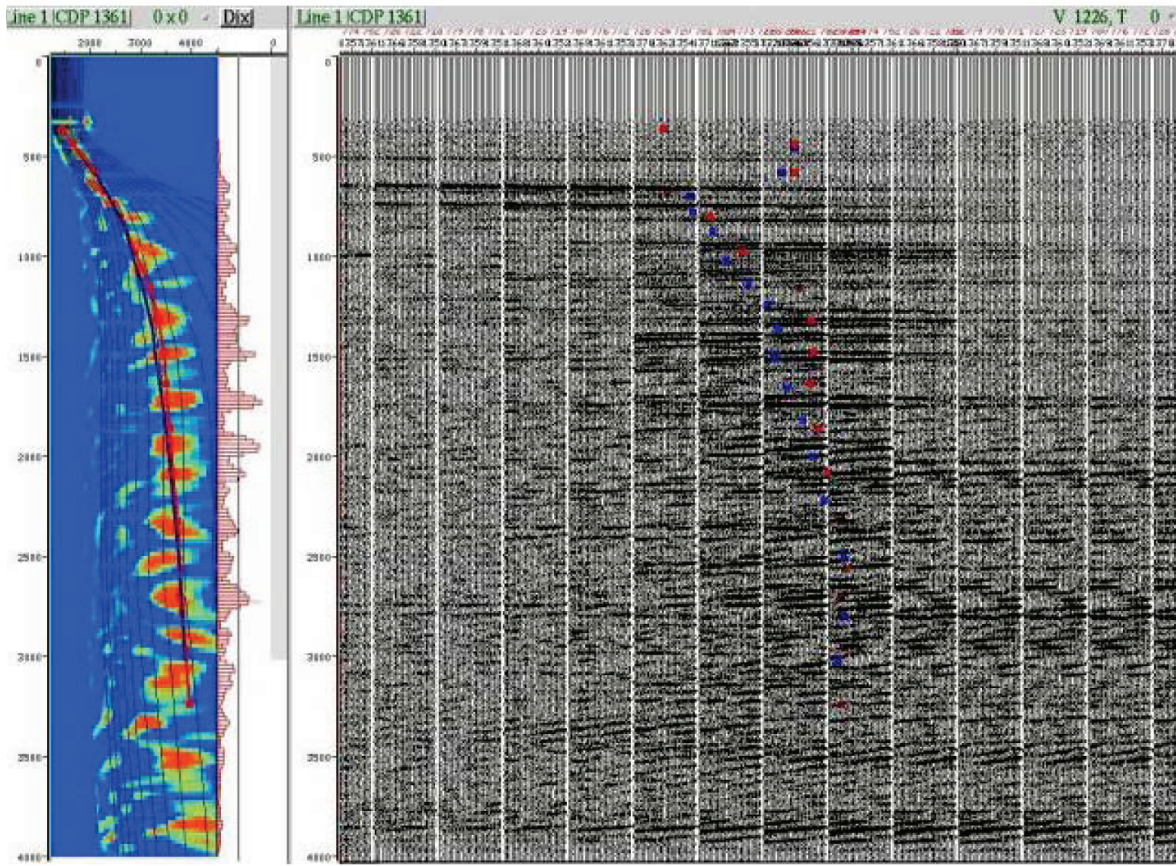


Fig. 7. Velocity spectrum.

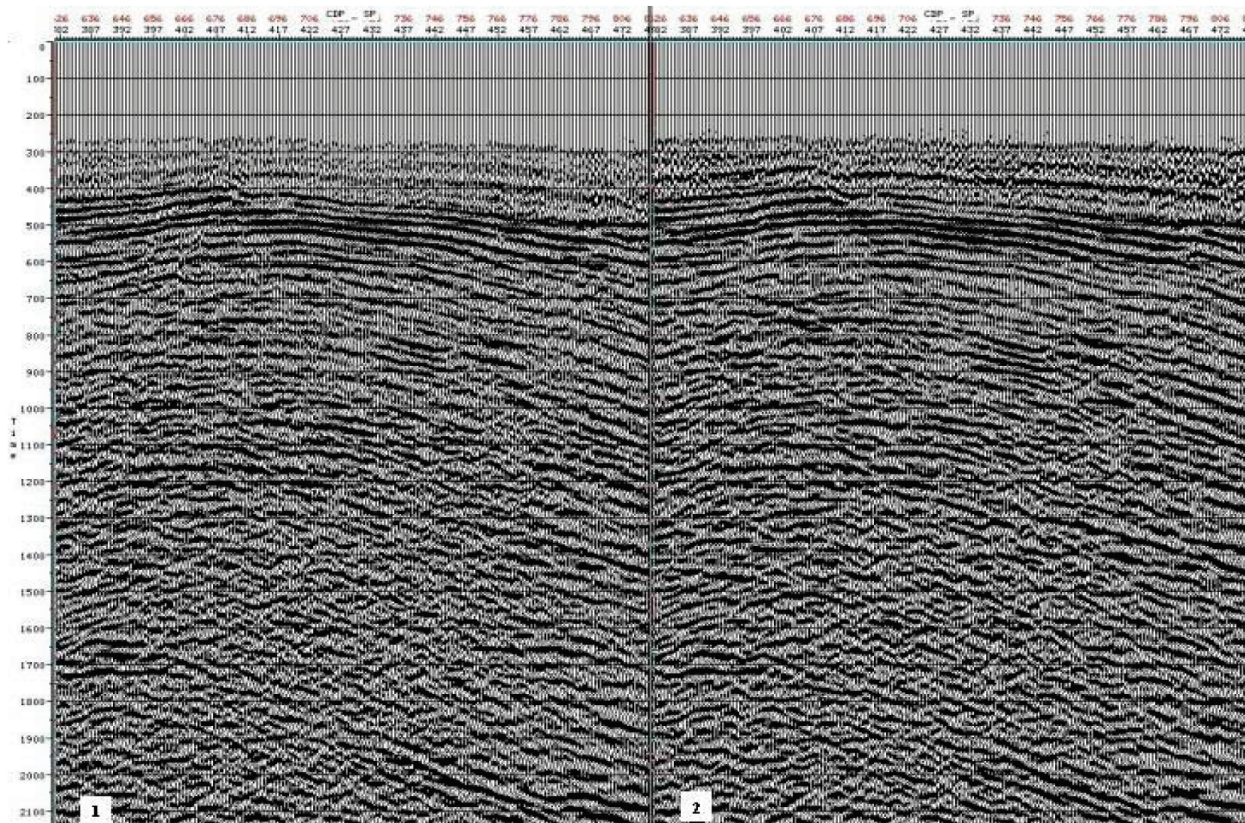


Fig. 8. Part of the stacked section showing: 1) without residual statics, and 2) with residual statics.



algorithm (Schneider, 1978). Data input to the DMO is in common offset order, has full static applied, and is NMO corrected with the 1km velocity field. The offsets were regularized to ensure each offset plane had a trace for each CMP.

The offset interval and DMO dip applied is: offset interval=80m, DMO dip=15 degrees. The DMO produced more significant effects on the steeper dipping data, but generally helped to improve the S/N ratio. (Fig. 9).

### Final Velocity Analysis

The final or second pass velocity analysis was picked at 1km intervals using groups 24 CMPS. The data was set to the near surface floating datum, and pre-processed with the DMO and band pass filter applied. The velocities were picked interactively, using variable velocity stacks, semblance, and gather displays.

### Second Pass Residual Statics

The same parameters were used as for the first pass of residual statics. The range of statics values from the second pass has never exceeded +/-5 ms.

### Variable Muting

Variable muting were picked and refined interactively. The data was re-stacked with the revised mute (Fig.10).

## POST STACK PROCESSING

### Time Variant (TV) Band-Pass Filter

A time variant band-pass filter was derived from filter scan test .The filter parameters are: Time=0 -1000 / 1000 -2800 ms and Filter=12-55 /12-45 Hz.

### Stack

Stack normalization/compensation scaling of the form  $1/\sqrt{N}$ , where N is the stacking fold, was applied in the stacking process.

### Final Scaling

Scaling function to balance and enhance the look of data was run. Automatic gain control (AGC)

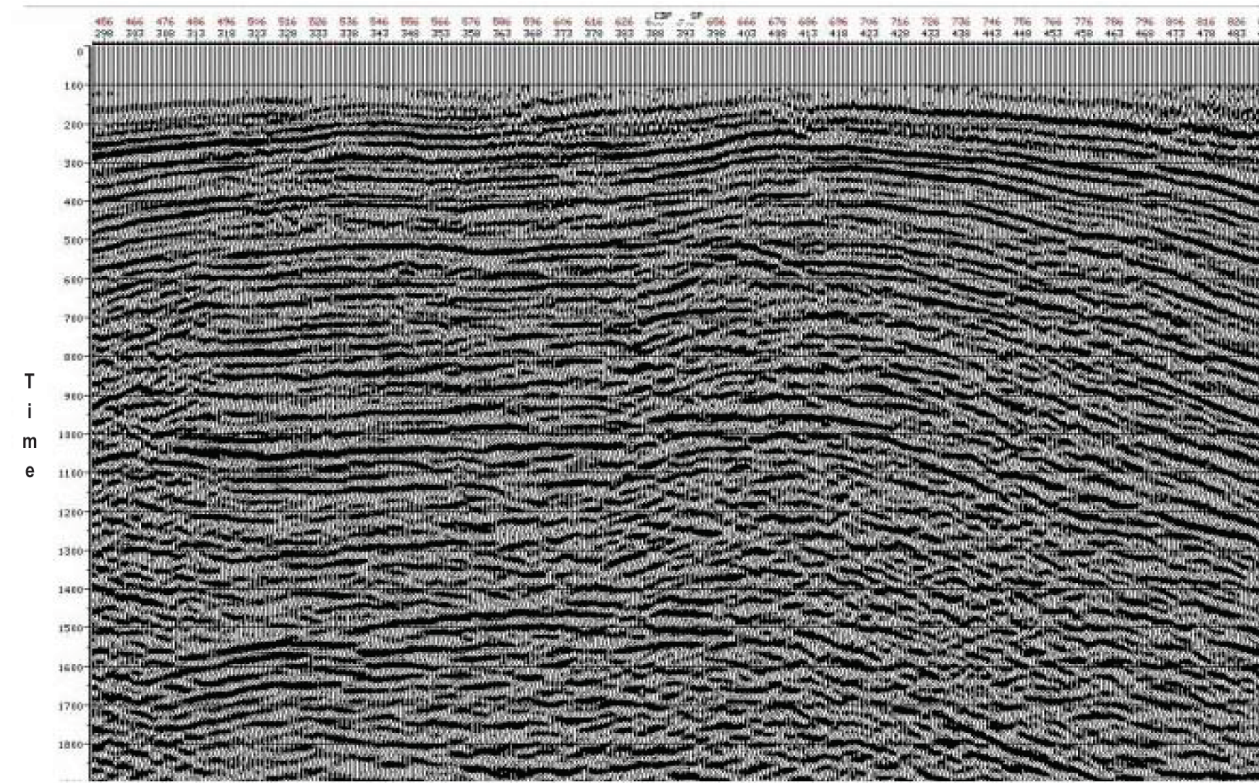


Fig. 9. Stack section of final DMO.



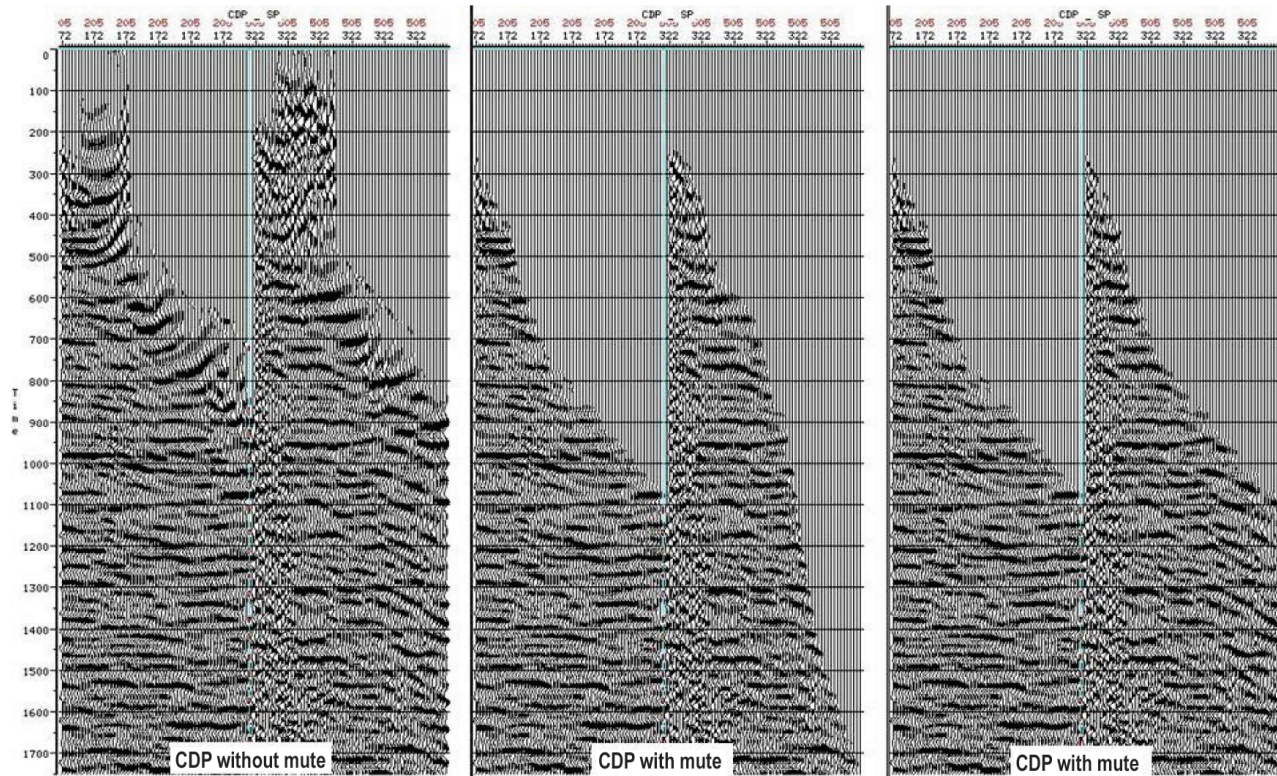


Fig. 10. Showing variable mute (middle) and constant mute (left).

scaling, trace balance (one and multi windows), AGC multi windows proved the most suitable.

The different scaling gates chosen are:

Time = 0-1000ms      AGC = 200ms.  
 = 1000-2800ms      = 600ms.

**Random Noise Attenuation in The F-X Domain.**

To attenuate the random noise in a spatial-temporal gate, without affecting the spatially coherent events, Frequency-Distance (FX) filtering is performed. The parameters selected as optimal is:

Window in traces= 30, Filter in traces= 9, Filter= 8-45Hz.

**Time Migration**

An initial set of tests was carried out to test migration algorithms. Finite-difference, FX and Kirchhoff-Time migrations were run. The Kirchhoff-Time migration carried a clear advantage for concession 72NW (Barrut Arch area).

The velocities (Fig.11) input to the migration were tested at various percentages of the final stacking velocities. Results showed that 95% for Concession 72 NW (Barrut Arch Area) is the best (Fig.12).

**SPECIAL TEST OF PRESTACK TIME MIGRATION (PSTM)**

Prestack Time Migration is a method of imaging seismic data and makes it appear similar to the real geologic cross-section. The Prestack time migration is the data migrated with correct stacking velocities and is a rigorous solution to the problem at conflicting dips. Kirchhoff Prestack migration is a commonly used algorithm for Prestack time migration. It provides high resolution, accurate imaginary and improved velocity estimation (Fig. 13a,b,c, and d). It involves splitting the process into four steps (Fig. 14).

The reprocessing final production parameters are listed below:

**REPROCESSING FINAL PRODUCTION PARAMETERS**

1. Input: Seg D input data  
     Sample rate =2ms length=5000ms 120 traces
2. Demultiplexing and gain removal
3. Editing
4. Geometry assignment
5. Amplitude recovery  $t^{**1.6}$
6. FK-filter full fan  
     Passing 4000 m/s



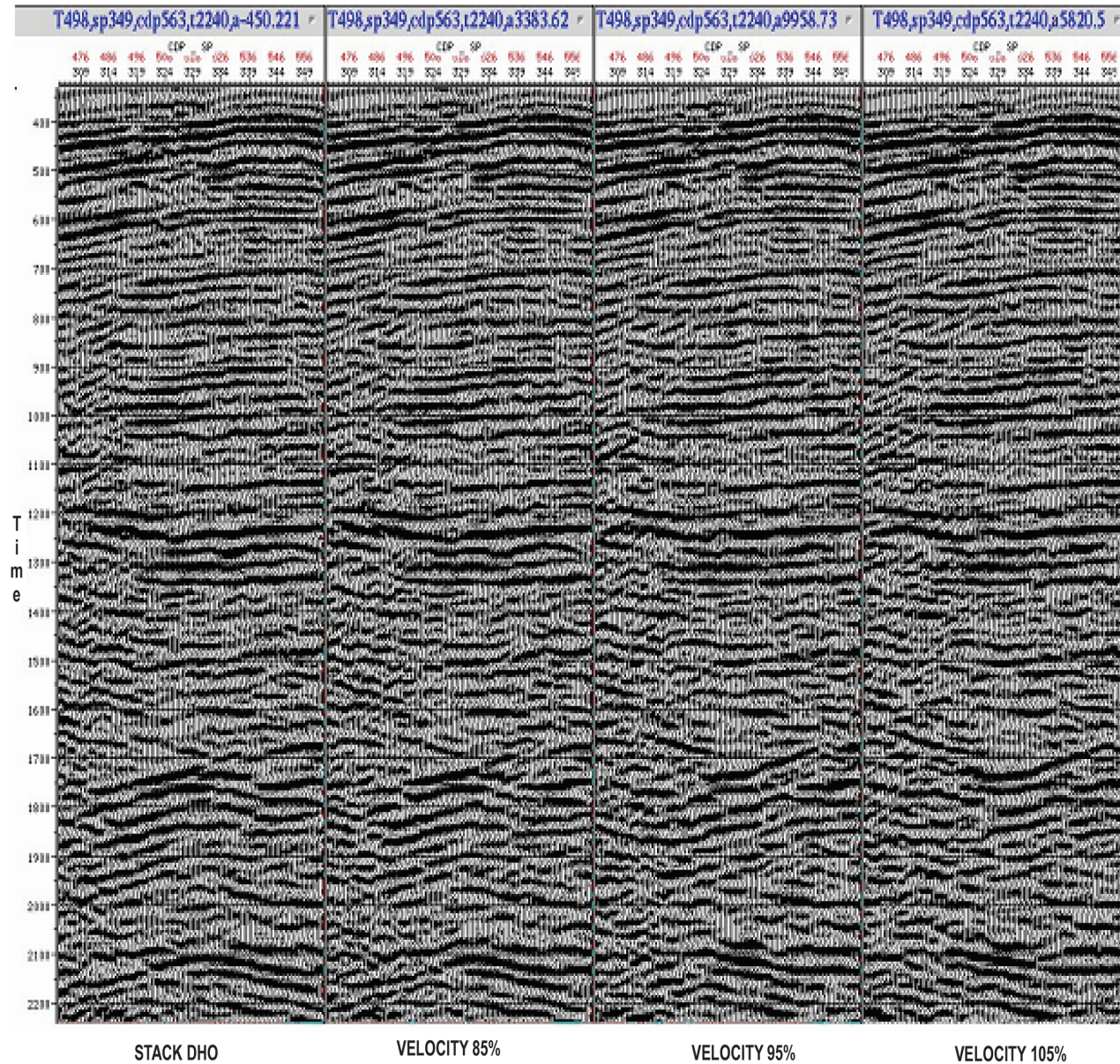


Fig. 11. Migration test at various percentages of the final stacking velocities.

- |                                     |  |
|-------------------------------------|--|
| 7. Surface Consistent Deconvolution | 11. Muting: variable muting            |
| Predictive algorithm                | 12. Dip moveout                        |
| Operator Length=160MS GAP=24MS      | Integral kirchhoff method              |
| Window 0-1200MS                     | 13. Stack nominal 60 fold              |
| Operator Length=160MS GAP=12MS      | 14. Datum static: datum level 200 m    |
| Window 900-2400MS                   | 15. Migration: Kirchhoff method        |
| 8. Refraction Static Correction     | Dz= 20 MS                              |
| Datum level : floating datum        | Using 95% stacking velocities          |
| Calculation : first break picking   | 16. Random Noise Attenuation           |
| Correction velocity: 2000 m/s       | FX-Deconvolution                       |
| 9. Automatic Surface Consistent     | Widow 60 traces Operator=19 traces     |
| Residual statics                    | 17. Filter: Type Band-pass             |
| Correction limit: 15 ms             | Travel time           low cut-High cut |
| Gate: 200-2800 ms                   | Sec                    Hz              |
| 10. Normal Moveout Correction       | 0 - 1.0               12 - 55          |
| Velocity analysis every 1200 m      | 1.0 - 2.8             12 - 45          |



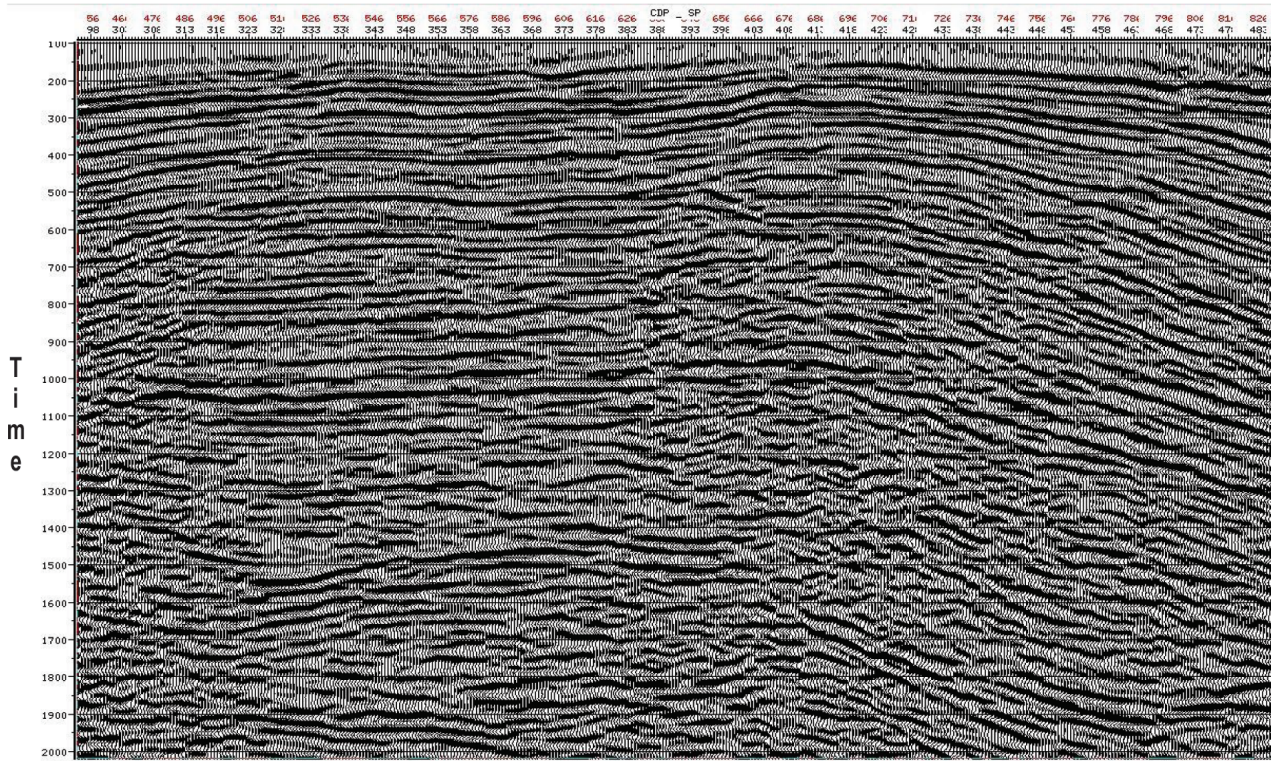


Fig. 12. CDP stack of final migration.

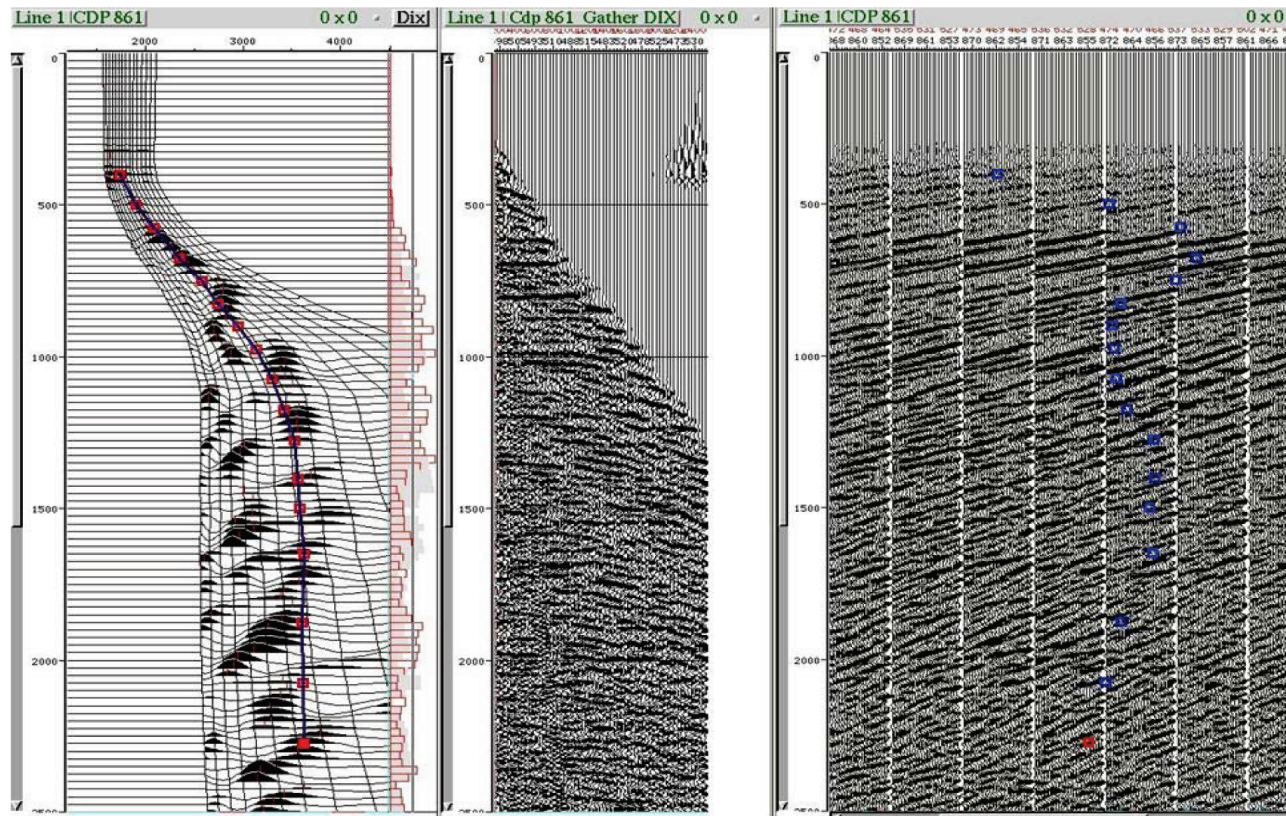


Fig. 13a. Velocity analysis before Prestack time migration at CDP 861.



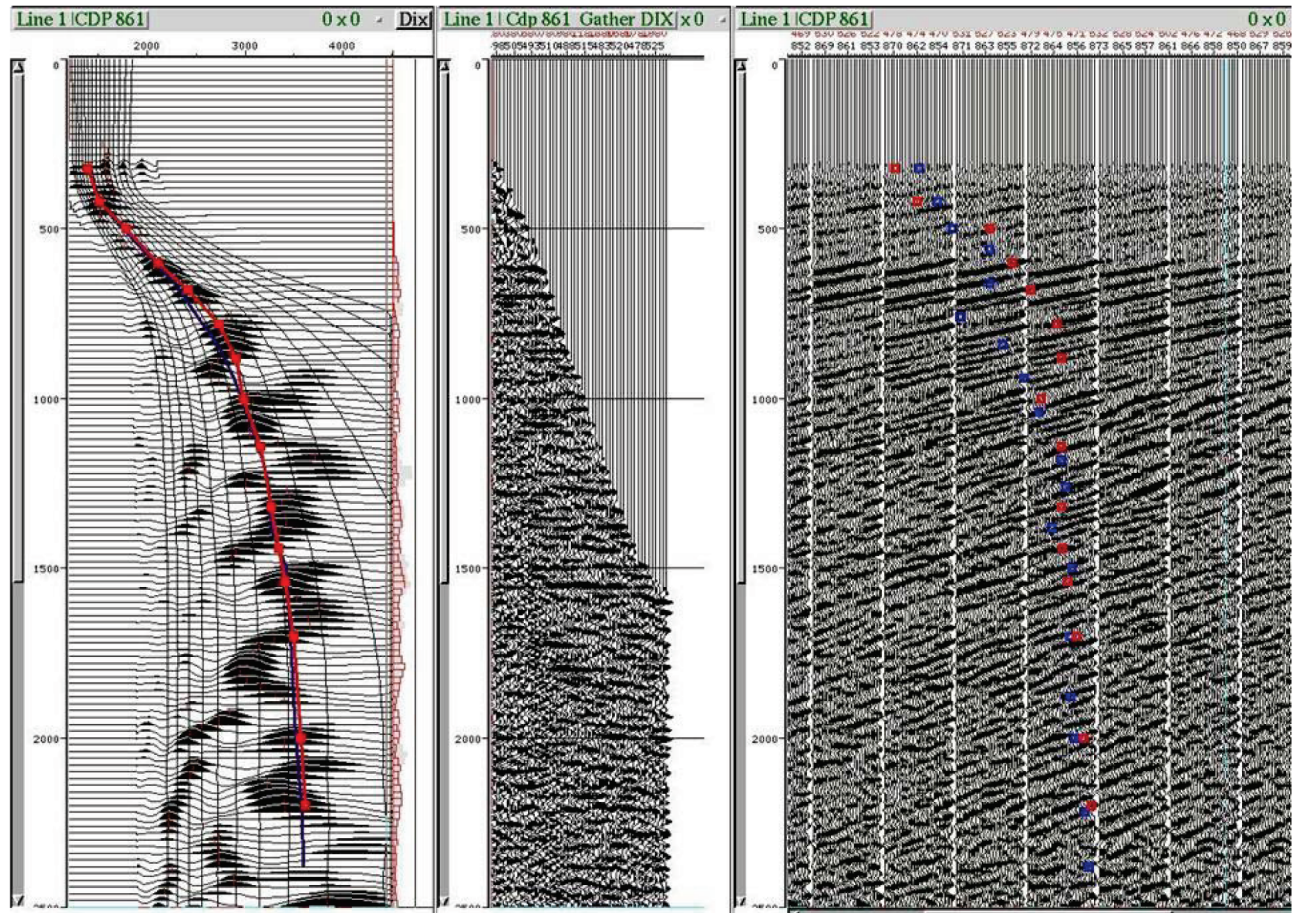


Fig. 13b. Velocity analysis after Prestack time migration at CDP 861.

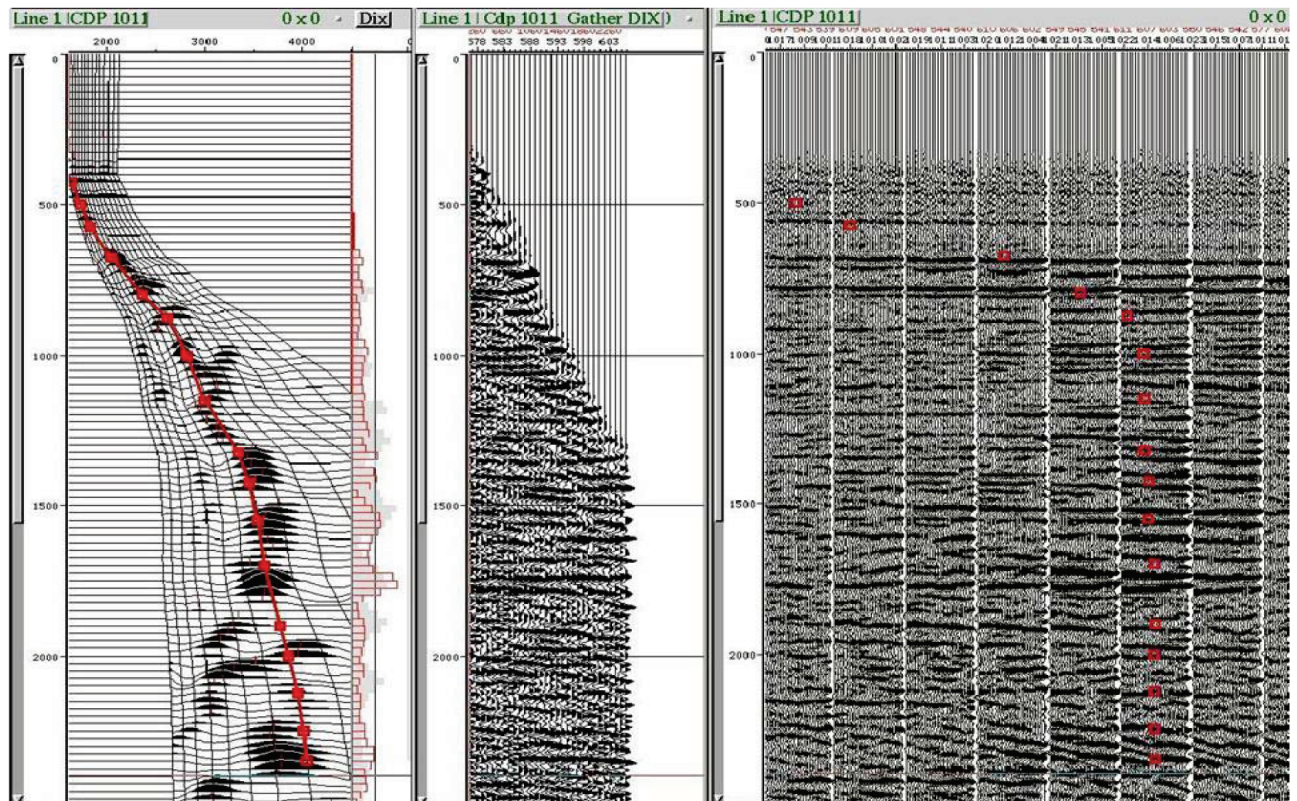


Fig. 13c. Velocity analysis before Prestack time migration at CDP1011.



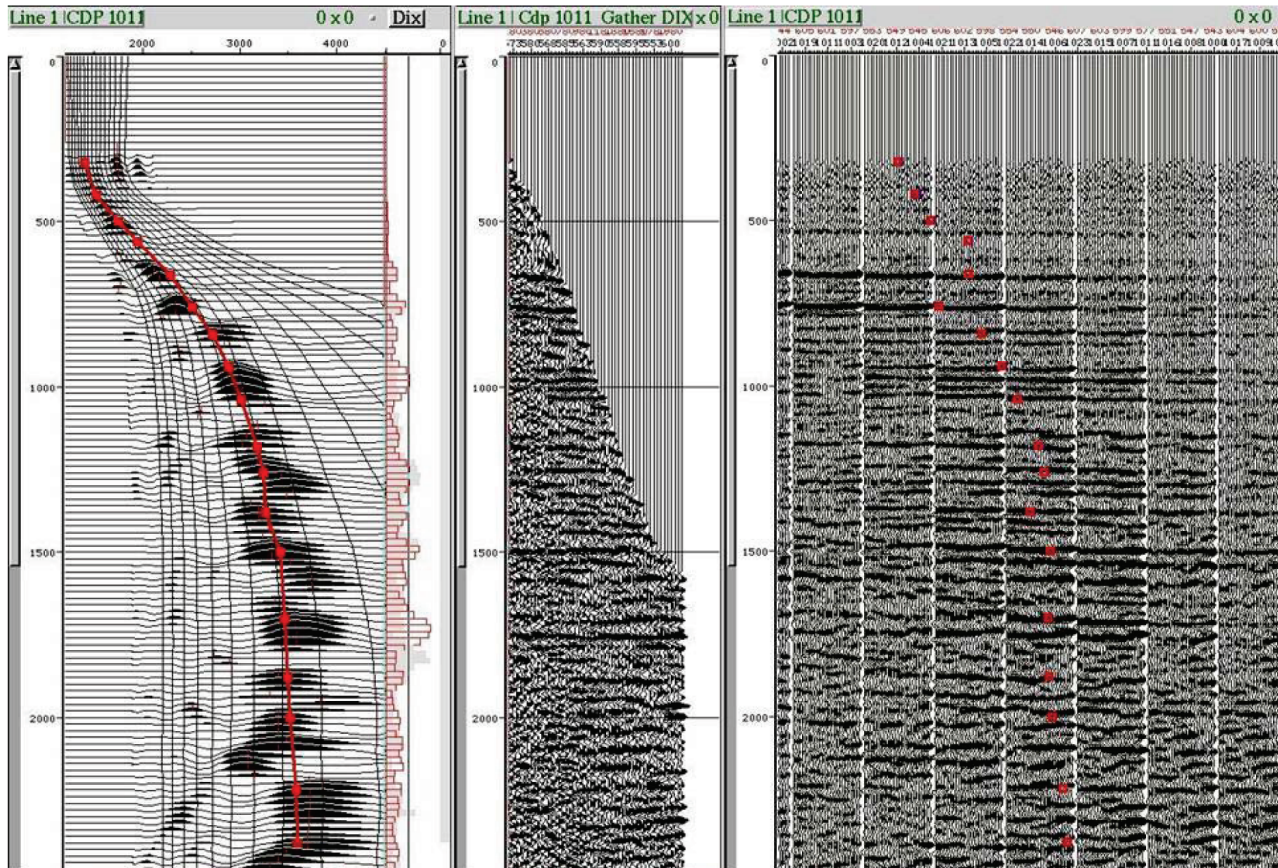


Fig. 13d. Velocity analysis after prestack time migration at CDP1011.

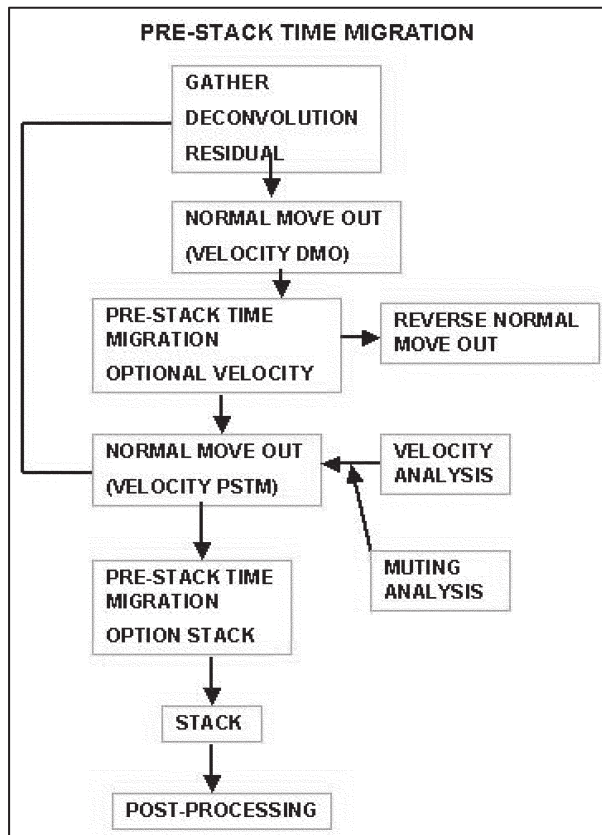


Fig. 14. Prestack time migration flow chart.

18. Equalisation:

- Window 0 - 1.0 Gate 200 ms.
- Window 1.0 - 2.8 Gate 600 ms.

### DISCUSSION OF RESULTS

The fundamental reason behind the reprocessing was to attempt to improve the imaging by using the latest algorithms and best possible seismic processing available. Incremental improvements in the image quality were expected and achieved. The reprocessing produced seismic sections with increased temporal and spatial resolution, facilitating more accurate interpretation of the data. The major difference in the production sequence between the original processing (Fig. 15a and b) and current processing (Fig.16) is attributed to the refraction tomography, Kirchhoff DMO, migration and F-X deconvolution. The processing methodology described in this paper resulted in seismic sections with increased interpretation confidence, which will aid in the understanding of the Barrut Arch deformation and improve the mapping of the structural subdivision shown in Figure 17. Figure 17 shows the stacked



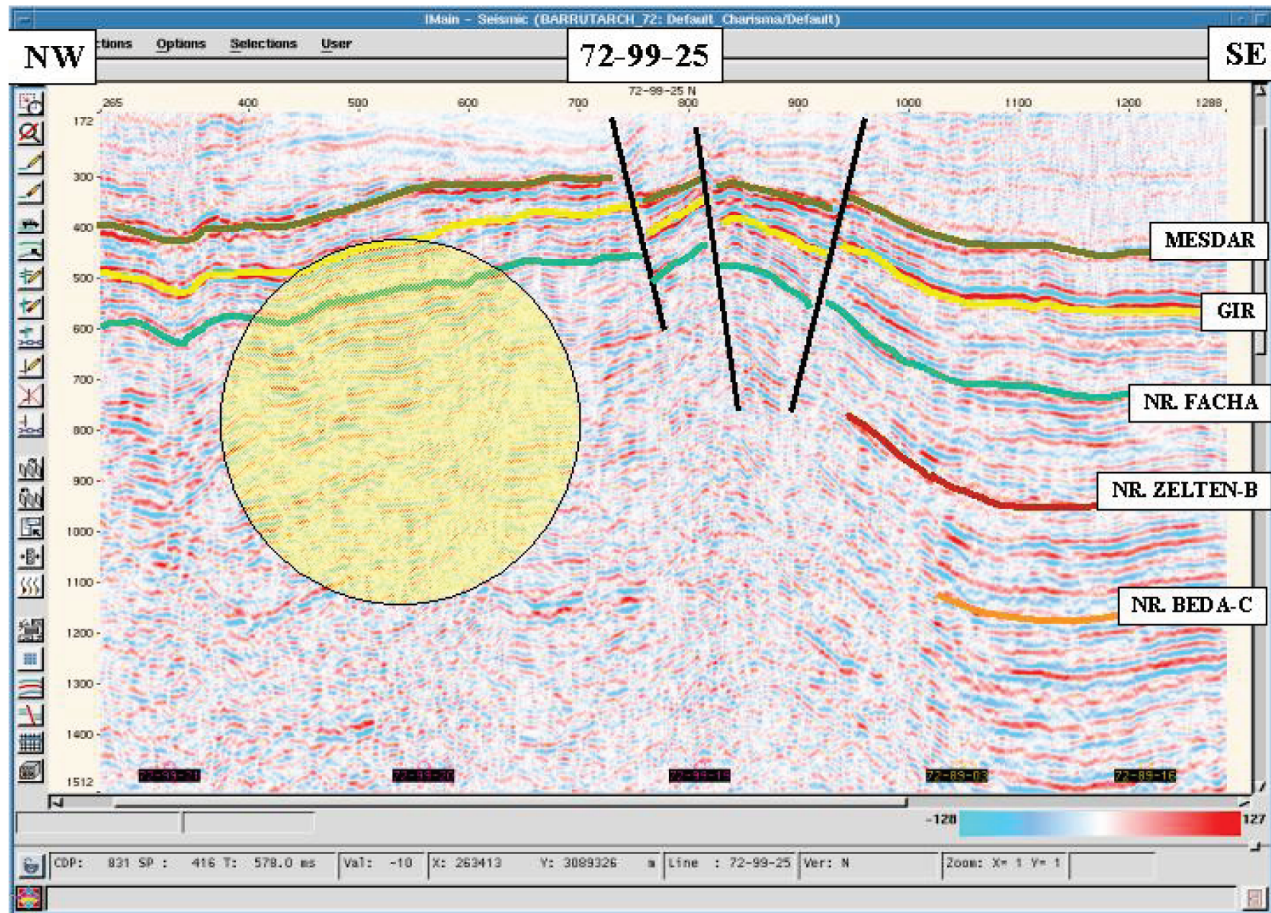


Fig. 15a. Poststack time migration of original processed line 72-99-25.

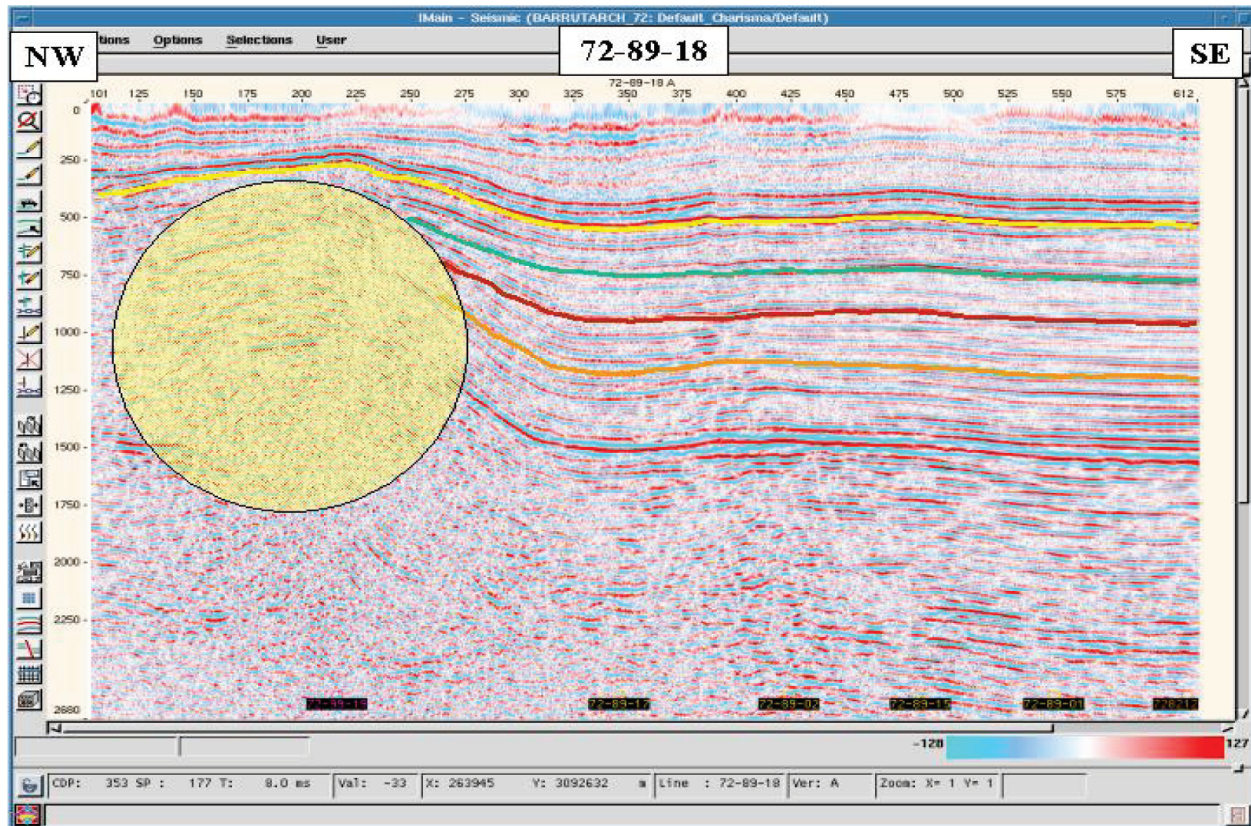


Fig. 15b. Poststack time migration of original processed line 72-89-18.



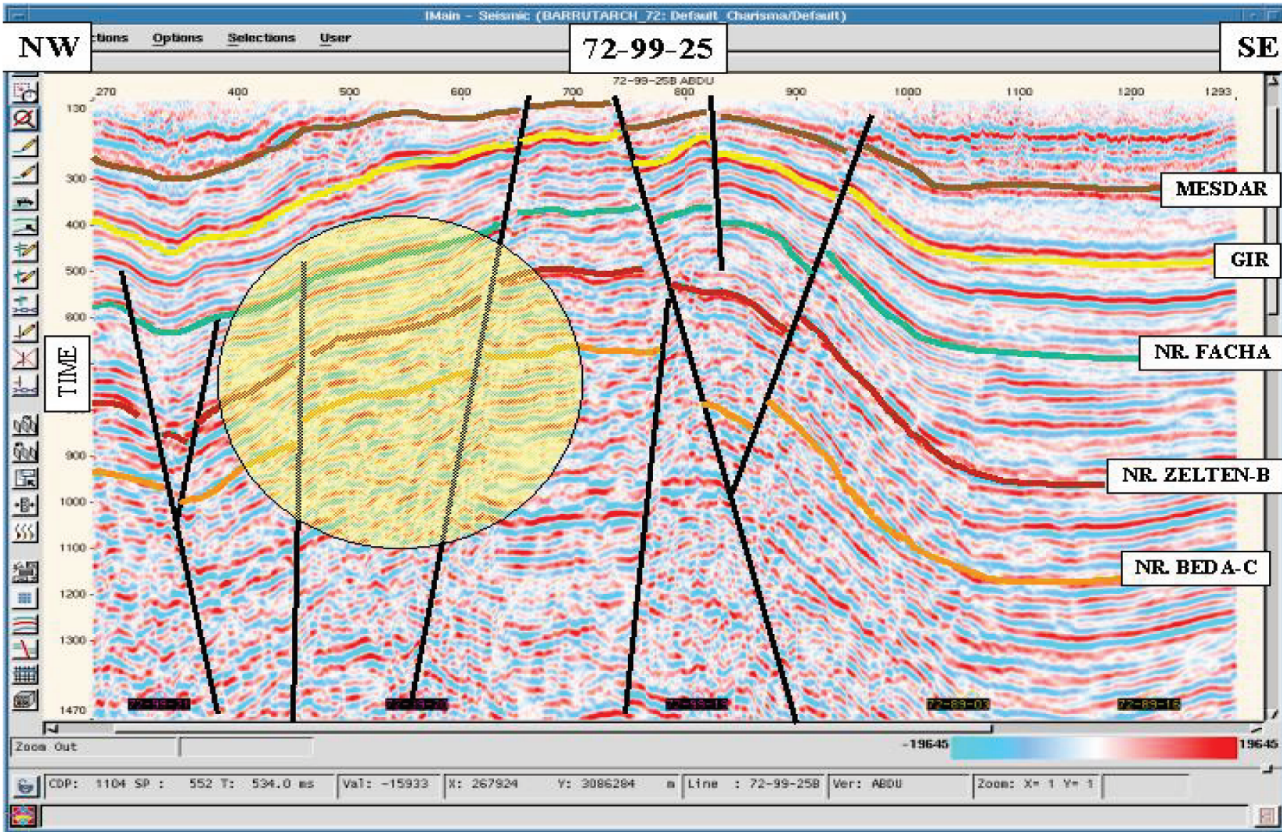


Fig. 16. Poststack time migration of reprocessed line 72-99-25.

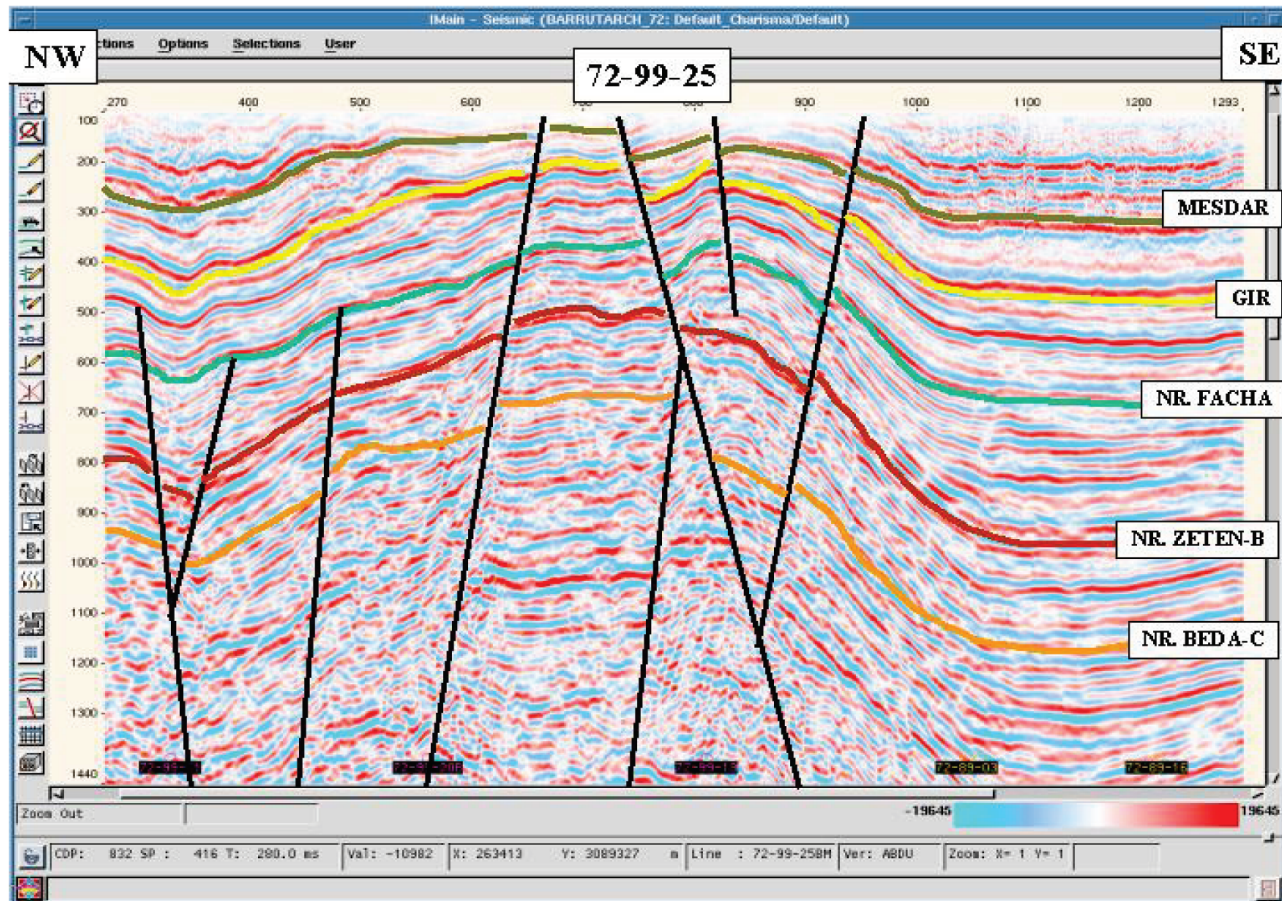


Fig. 17. Prestack time migration of reprocessed line 72-99-25.



section after Prestack time migration. Prestack time migration provided only minor improvement in seismic resolution in comparison with the post stack time migration with F-X deconvolution. Post stack time migration was chosen therefore because this is much more cost effective. Further interpretation of the reprocessed data will also add considerable value to the evaluation of the hydrocarbon potential of the Barrut Arch and may provide some prospective trends for future petroleum exploration.

### CONCLUSIONS

- 1 – Reprocessing of the seismic sections yielded significant improvement over the earlier processed data.
- 2 – Reprocessing of old data can help in enhancing detail and so should be considered more often.
- 3 – Seismic reprocessing becomes a very important and relatively cheap alternative to the acquisition of new seismic data as proved in this work.
- 4 – Seismic reprocessing enhances data quality and ensure confident seismic interpretation, integration with other geosciences data may provide a new impetus for oil and gas exploration along the Barrut Arch area.
- 5 – The reprocessing produced seismic sections with increased temporal and spatial seismic resolution. This technique provides cost effective results, facilitating more accurate interpretation of the data. Enhanced imaging of the fault pattern and definition as well as the formation sequences has been achieved; this should aid the understanding of rock deformation and improve the mapping of structural subdivisions within the Barrut Arch.
- 6 – This area needs to be surveyed with 3D seismic data with high enough fold, frequency and quality to allow the desired analysis.

### ACKNOWLEDGEMENT

The authors would like to thank the management and the Exploration Department of Veba Oil Operations for making all the data available to us, we also acknowledge their help and encouragement with gratitude.

### REFERENCES

- Banar, F.J., 1967. *Surface and Uphole Geology, Northwest Barrut: LGM 92*, Mobil Oil Libya Ltd., Internal report.
- Geophoto Libya Inc., 1959. *Photogeologic Evaluation, Concession 72 Libya: LIB 60*, Mobil Oil of Canada Ltd., (Libyan Branch), internal report.
- Johnson, J.T., and Gates, J.K., 1959. *Geology of El Barrut Anticline (Southern Part) Concession No. 72, and Zone iv, Libya: LIB 73*, Mobil Oil of Canada Ltd., (Libyan Branch), Internal report.
- Johnson, B.A.1992. *Geological Evaluation of Concession 72: LGM 179*, Veba Oil Operations, Internal Report.
- Raodifar, R.E.1958. *The Reconnaissance Geological Survey of Mobil Oil Concession no. 72. Libya; LIB 27*, Mobil Oil of Canada Ltd., (Libyan Branch), Internal report.
- Schneider, W.A., 1978. Integral formulation for migration in two and three dimensions. *Geophysics*, **43**, 49-76.
- Yilmaz, O., 1987. *Seismic Data Processing*. Society of Exploration Geophysics, Ed. Stephen M. Doherty.